

# Practical and Thermodynamic Constraints on Electromicrobially-Accelerated CO<sub>2</sub> Mineralization

Sabrina Marecos<sup>1</sup>, Rae Brigham<sup>1</sup>, Anastacia Dressel<sup>1\*</sup>, Larissa Gaul<sup>1\*</sup>, Linda Li<sup>1\*</sup>, Krishnathreya Satish<sup>1\*</sup>, Indira Tjokorda<sup>1\*</sup>, Jian Zheng<sup>1\*</sup>, Alexa M. Schmitz<sup>1</sup>, and Buz Barstow<sup>1†</sup>

<sup>1</sup>Department of Biological and Environmental Engineering, Cornell University, Ithaca, NY 14853, USA

\*These authors contributed equally to this article.

†Corresponding author:

Buz Barstow, 228 Riley-Robb Hall, Cornell University, Ithaca, NY 14853; [bmb35@cornell.edu](mailto:bmb35@cornell.edu)

## Abstract

By the end of the century tens of gigatonnes of CO<sub>2</sub> will need to be removed from the atmosphere every year to maintain global temperatures. Natural weathering of ultramafic rocks and subsequent mineralization reactions can convert atmospheric CO<sub>2</sub> into ultra-stable carbonates. But, while natural weathering will eventually draw down all excess CO<sub>2</sub>, this process will need hundreds of thousands of years to do it. The CO<sub>2</sub> mineralization process could be accelerated by weathering ultramafic rocks with biodegradable lixiviants like organic acids. But, in this article we show that if these lixiviants are produced from cellulosic biomass, the demand created by CO<sub>2</sub> mineralization could monopolize the world's supply of biomass even if CO<sub>2</sub> mineralization performance is high. In this article we demonstrate that electromicrobial production technologies (EMP) that combine renewable electricity and microbial metabolism could produce lixiviants for as little as \$200 to \$400 per tonne at solar electricity prices achievable within the decade. Furthermore, this allows the lixiviants needed to sequester a tonne of CO<sub>2</sub> to be produced for less than \$100, even with modest CO<sub>2</sub> mineralization performance.

## Introduction

The IPCC's (Intergovernmental Panel on Climate Change) 2018 special report on the impact of climate change highlighted the need for significant deployment of negative emissions technologies to limit global warming [ipcc2018a]. The IPCC estimates that by the end of the 21st century,  $\approx 20$  gigatonnes of CO<sub>2</sub> (GtCO<sub>2</sub>) will need to be removed from the atmosphere every year to limit global temperature rise to 1.5 °C [ipcc2018a].

Of all the negative emissions technologies examined for large scale CO<sub>2</sub> removal, carbon mineralization has the largest potential storage capacity [Keleman2019a, Beerling2020a, Lehmann2020a]. The CO<sub>2</sub> storage capacity of carbon mineralization in ultramafic systems is truly enormous. For example, peridotite reservoirs across the globe (largely containing the mineral olivine) have the potential to mineralize and sequester 10<sup>5</sup>-10<sup>8</sup> GtCO<sub>2</sub> [Keleman2019a], between 100 and 100,000 × the excess CO<sub>2</sub> in the atmosphere (there are  $\approx 600$  Gt more CO<sub>2</sub> in the atmosphere than in pre-industrial times, and  $\approx 430$  Gt more CO<sub>2</sub> in the oceans [NOAA2021a]).

Natural weathering of exposed sections of mantle rocks will eventually draw down all excess CO<sub>2</sub> in the atmosphere, but will take thousands of years to do it [Archer2009a].

Mineral-dissolving microbes could accelerate mineral weathering. However, almost all mineral-dissolving microbes need to be powered by the degradation of plant biomass (*i.e.*, the product of photosynthesis). For example, the mineral-dissolving microbe *Gluconobacter oxydans* B58 oxidizes the sugar glucose to the environmentally benign lixiviant (a mineral-dissolving compound) gluconic acid (glucose can be derived from degradation of cellulose, one of the primary components of biomass) [Reed2016a, Schmitz2021b].

However, the world's growing [Prosekov2018a] and increasingly wealthy population [PwC2015a] is creating a growing need for arable land [Tilman2011a], tightening the world's biomass supply [Slade2014a]. Could the use of plant biomass to power CO<sub>2</sub> mineralization compete with the world's food supply?

Electromicrobial production (EMP) could enable production of lixiviants for CO<sub>2</sub> mineralization without competing with the world's biomass supply. EMP technologies [Rabaey2010a, Rabaey2011a, Lips2018a, Salimijazi2019a, Claassens2019a, Prevotau2020a] that combine biological and electronic components have been demonstrated at lab scale to have energy to chemical conversion efficiencies exceeding all forms of terrestrial photosynthesis [Liu2016a, Haas2018a], while theoretical predictions indicate that their efficiency could exceed all forms of photosynthesis [Claassens2019a, Salimijazi2020b, Leger2021a, Wise2021a]. Globally, photosynthesis has an average solar to biomass conversion of less than 1% [Barstow2015a]. In contrast, lab scale experiments have demonstrated a solar to product conversion efficiency of  $\approx 10\%$  for EMP [Liu2016a], while theoretical predictions indicate that this could rise to over 15% [Salimijazi2020b]. This order of magnitude increase in solar to product conversion efficiency could allow the production of lixiviants with no competition for arable land or wilderness.

In this article, we present a simplified model that estimates the global need for lixiviants for CO<sub>2</sub> mineralization, the costs of synthesizing these lixiviants by electromicrobial production, and the costs of sequestering 1 tonne of CO<sub>2</sub> using electromicrobially produced lixiviants.

## Theory

A full set of symbols used in this article is included in **Table 1**.

### Simplified Carbon Mineralization Reactions and Lixiviant Need

How much lixiviant is required to capture 20 GtCO<sub>2</sub> per year (the approximate quantity estimated by the IPCC in order to limit global temperature rise to  $\approx 1.5$  °C [ipcc2018a])? To simplify the calculation, we consider just the conversion of magnesium olivine (forsterite) into magnesium carbonate (magnesite) through a two-step reaction. In the first step, solid forsterite is dissolved to aqueous (aq) magnesium ions [Power2013a],



In a later precipitation reaction, these Mg<sup>2+</sup> ions react with atmospheric CO<sub>2</sub> and precipitate as stable solid (s) carbonates including magnesite (MgCO<sub>3</sub>) [Power2013a],



How much forsterite needs to be dissolved to capture 20 GtCO<sub>2</sub>? The maximum number of CO<sub>2</sub> molecules (or C atoms) that can be sequestered by the dissolution of a single asymmetric unit of forsterite (Mg<sub>2</sub>SiO<sub>4</sub>),  $n_{C, \text{olivine}}$ , is 2 (one asymmetric unit of forsterite contains 2 Mg atoms, which can each react with 1 carbon atom). The molecular weight of a single forsterite asymmetric unit is 141 grams per mole, and the molecular weight of 2 C atoms is 24 grams per mole. Thus, the minimum mass of forsterite needed to capture a mass of carbon  $M_C$  (e.g., 0.27 GtC corresponding to 1 GtCO<sub>2</sub>), is,

$$\frac{M_{\text{forsterite}}}{M_C} = \frac{\text{MW}_{\text{forsterite}}}{\text{MW}_C n_{C, \text{forsterite}}} \quad (3)$$

Therefore, to sequester 1 gigatonne of CO<sub>2</sub>, at least 16 gigatonnes of forsterite need to be dissolved [Power2013a].

How much lixiviant is needed to dissolve this much forsterite? The volume of the forsterite can be simply calculated from its density,  $\rho_{\text{forsterite}}$ ,

$$V_{\text{forsterite}} = M_{\text{forsterite}} / \rho_{\text{forsterite}} \quad (4)$$

The volume of the lixiviant,  $V_{\text{lix}}$ , can be calculated from the experimentally-derived pulp density that gives the best mineral dissolution,

$$\rho_{\text{pulp}} = M_{\text{forsterite}} / V_{\text{lix}} \quad (5)$$

$\rho_{\text{pulp}}$  is typically expressed in % w/v. For example,  $\rho_{\text{pulp}} = 2\%$ , means that 2 grams of forsterite are dissolved in 100 mL of lixiviant. However, so that we can use the experimentally derived pulp density along with our preferred units, we express  $\rho_{\text{pulp}}$  in terms of g m<sup>-3</sup> (simply multiply  $\rho_{\text{pulp}}$  in w/v by 10<sup>4</sup>).

The mass of the dry lixiviant can be calculated simply from its molecular weight; concentration,  $c_{\text{lix}}$ ; and volume,  $V_{\text{lix}}$ ,

$$M_{\text{lix}} = \text{MW}_{\text{lix}} c_{\text{lix}} V_{\text{lix}} \quad (6)$$

A full listing of molecular weights of the lixiviant compounds considered in this article is included in **Table S1**.

Thus, the minimum mass of the lixiviant needed to dissolve  $M_{\text{forsterite}}$ , and hence to sequester  $M_C$  of carbon is,

$$M_{\text{lix}} \geq \frac{M_C \text{MW}_{\text{forsterite}} c_{\text{lix}} \text{MW}_{\text{lix}}}{\text{MW}_C n_{C, \text{forsterite}} \rho_{\text{pulp}}} \quad (7)$$

However, not all steps in the CO<sub>2</sub> mineralization process will be perfectly efficient. The extraction of Mg from forsterite will be imperfect (**Equation 1**), as will the later precipitation of Mg<sup>2+</sup> ions as a carbonate (**Equation 2**). To account for this, we introduce extraction efficiency,  $\eta_{\text{ex}}$ , and precipitation efficiency,  $\eta_{\text{precip}}$ ,

$$M_{\text{lix}} = \frac{M_C \text{MW}_{\text{forsterite}} c_{\text{lix}} \text{MW}_{\text{lix}}}{\text{MW}_C n_{C, \text{forsterite}} \eta_{\text{ex}} \eta_{\text{precip}} \rho_{\text{pulp}}}. \quad (8)$$

The formula for the mass of lixiviant,  $M_{\text{lix}}$ , required to sequester a given amount of carbon per year, is composed of two sets of terms: those with at least reasonably well known values ( $\text{MW}_{\text{forsterite}}$ ,  $\text{MW}_C$ ,  $n_{C, \text{forsterite}}$ ), and a second set whose values have high uncertainty ( $\eta_{\text{ex}}$ ,  $\eta_{\text{precip}}$ ,  $\rho_{\text{pulp}}$ ,  $c_{\text{lix}}$ ),

$$M_{\text{lix}} = \underbrace{\frac{M_C \text{MW}_{\text{forsterite}} \text{MW}_{\text{lix}}}{\text{MW}_C n_{C, \text{forsterite}}}}_{\text{high certainty terms}} \times \underbrace{\frac{c_{\text{lix}}}{\eta_{\text{ex}} \eta_{\text{precip}} \rho_{\text{pulp}}}}_{\text{high uncertainty terms, } \zeta}. \quad (9)$$

We denote the product of the high uncertainty terms as  $\zeta$ , the inverse CO<sub>2</sub> mineralization performance. The higher  $\zeta$  gets, the more lixiviant it takes to sequester  $M_C$ . Given that the uncertainty in each of the four terms in  $\zeta$  is equally high, we choose to make our estimate of  $M_{\text{lix}}$  a function of  $\zeta$  rather than any single uncertain parameter. Thus,

$$M_{\text{lix}} = \frac{M_C \text{MW}_{\text{forsterite}} \text{MW}_{\text{lix}}}{\text{MW}_C n_{C, \text{forsterite}}} \zeta. \quad (10)$$

### Theory of Electromicrobial Production

We have extended our theoretical framework for calculating the efficiency of electromicrobial production (EMP) [Salimijazi2020b, Wise2021a] to calculate the energy cost of lixiviant production from renewable electricity and CO<sub>2</sub>. Full derivations of the equations presented here can be found in the supplement to our original electromicrobial production efficiency theory article (Salimijazi *et al.* [Salimijazi2020b]), and in our recent work on electromicrobial production of protein with extends our theory to calculate the energy (electrical or solar) costs of producing a gram of product (Wise *et al.* [Wise2021a]).

We consider a bio-electrochemical system used to deliver electrons to microbial metabolism (**Fig. 1B**). Electrical power is used to generate lixiviant molecules with a molecular weight  $\text{MW}_{\text{lix}}$ . The amount of electricity needed to produce a unit-mass of the lixiviant is,

$$C_{\text{Elix}} \geq N_A \Delta U_{\text{cell}} e \nu_{\text{elix}} / \text{MW}_{\text{lix}}, \quad (11)$$

where  $e \nu_{\text{elix}}$  is the amount of charge needed to synthesize a single lixiviant molecule from CO<sub>2</sub> (the fundamental charge,  $e$ , multiplied by the number of electrons needed for synthesis,  $\nu_{\text{elix}}$ );  $\Delta U_{\text{cell}}$  is the potential difference across the bio-electrochemical cell; and  $N_A$  is the Avogadro constant. A derivation of **Equation 11** can be found in Wise *et al.* [Wise2021a], building upon derivations in Salimijazi *et al.* [Salimijazi2020b].

For systems where CO<sub>2</sub> reduction is performed electrochemically, and the resulting reduction product (typically a C<sub>1</sub> compound like formic acid) [Appel2013a, White2014a, White2015a] is further reduced enzymatically,  $\nu_{\text{elix}}$  is substituted for number of electrons needed to convert the C<sub>1</sub> product into the lixiviant,  $\nu_{\text{elix, add}}$  [Salimijazi2020b],

$$C_{\text{Elix}} \geq \frac{e \nu_{\text{elix, add}} N_A \left( \Delta U_{\text{cell1}} \left( \frac{\nu_r \nu_{\text{er}} \nu_{\text{Cr}} \xi_{\text{I2}}}{\xi_{\text{I1}} \xi_{\text{C}} \nu_{\text{elix, add}}} \right) + \Delta U_{\text{cell2}} \right)}{\text{MW}_{\text{lix}} \xi_{\text{I2}}}, \quad (12)$$

where  $\nu_r$  is the number of primary reduction products (*i.e.*, formic acid molecules) needed to synthesize a molecule of the final product,  $\nu_{\text{er}}$  is the number of electrons needed to reduce CO<sub>2</sub> to a primary reduction product (*i.e.*, 2 in the case of formic acid),  $\nu_{\text{Cr}}$  is the number of carbon atoms per primary fixation product (*i.e.*, 1 in the case of formic acid),  $\xi_{\text{I2}}$  is the Faradaic efficiency of the bio-electrochemical cell,  $\xi_{\text{I1}}$  is the Faradaic efficiency of the primary abiotic cell 1,  $\xi_{\text{C}}$  is the carbon transfer efficiency from cell 1 to cell 2. A derivation of **Equation 12** can be found in Wise *et al.* [Wise2021a].

We calculate the electron requirements for lixiviant synthesis,  $\nu_{\text{elix}}$  (from CO<sub>2</sub>) or  $\nu_{\text{elix, add}}$  (from an electrochemical CO<sub>2</sub> reduction product), from the number of NAD(P)H ( $\nu_{\text{lix, NADH}}$ ) reduced Ferredoxin (Fd<sub>red</sub>;  $\nu_{\text{lix, Fd}}$ ) and ATP ( $\nu_{\text{lix, ATP}}$ ) molecules needed for the synthesis of the molecule, along with a model of the mechanism used for electron delivery to the microbe [Salimijazi2020b].

For systems that rely upon H<sub>2</sub>-oxidation for electron delivery like the Bionic Leaf [Torella2015a, Liu2016a],

$$\nu_{\text{elix, H}_2} = 2\nu_{\text{lix, NADH}} + 2\nu_{\text{lix, Fd}} + \nu_{\text{lix, ATP}} \frac{\text{ceil}(\Delta G_{\text{ATP/ADP}}/e \Delta U_{\text{membrane}})}{\text{floor}\left(\left(U_{\text{H}_2} - U_{\text{acceptor}}\right)/\Delta U_{\text{membrane}}\right)}, \quad (13)$$

where  $\Delta G_{\text{ATP/ADP}}$  is the free energy required for regeneration of ATP,  $\Delta U_{\text{membrane}}$  is the potential difference across the cell's inner membrane due to the proton gradient,  $U_{\text{H}_2}$  is the standard potential of proton reduction to H<sub>2</sub>,  $U_{\text{acceptor}}$  is the standard potential of terminal electron acceptor reduction (typically O<sub>2</sub> + 2e<sup>-</sup> to H<sub>2</sub>O), the ceil function rounds up the nearest integer, and the floor function rounds down to the nearest integer. A full derivation of **Equation 13** can be found in Section 2 (Equations 10 to 20) of the supplement for Salimijazi *et al.* [Salimijazi2020b].

The inner membrane potential difference,  $\Delta U_{\text{membrane}}$ , is the largest source of uncertainty in this calculation. Therefore, we present a range of efficiency estimates in **Figure 3** and throughout the text for  $\Delta U_{\text{membrane}} = 80$  mV (BioNumber ID (BNID) 10408284 [Milo2010a]) to 270 mV (BNID 107135), with a central value of 140 mV (BNIDs 109774, 103386, and 109775).

For systems that rely upon EEU for electron delivery like *Shewanella oneidensis* [Rowe2021a, Salimijazi2020b],

$$\begin{aligned}
 \nu_{\text{elix, EEU}} = & 2\nu_{\text{lix, NADH}} + 2\nu_{\text{lix, Fd}} \\
 & + \nu_{\text{lix, ATP}} \frac{\text{ceil}(\Delta G_{\text{ATP/ADP}}/e \Delta U_{\text{membrane}})}{\text{floor}\left(\left(U_{\text{Q}} - U_{\text{acceptor}}\right)/\Delta U_{\text{membrane}}\right)} \\
 & + \nu_{\text{lix, NADH}} \frac{\text{ceil}\left(\left(U_{\text{NADH}} - U_{\text{Q}}\right)/\Delta U_{\text{membrane}}\right)}{\text{floor}\left(\left(U_{\text{Q}} - U_{\text{acceptor}}\right)/\Delta U_{\text{membrane}}\right)} \\
 & + \nu_{\text{lix, Fd}} \frac{\text{ceil}\left(\left(U_{\text{Fd}} - U_{\text{Q}}\right)/\Delta U_{\text{membrane}}\right)}{\text{floor}\left(\left(U_{\text{Q}} - U_{\text{acceptor}}\right)/\Delta U_{\text{membrane}}\right)},
 \end{aligned} \tag{14}$$

where  $U_{\text{Q}}$  is the redox potential of the inner membrane electron carrier, thought to be ubiquinone [Rowe2018a],  $U_{\text{NADH}}$  is the standard potential of NAD(P)H, and  $U_{\text{Fd}}$  is the standard potential of Ferredoxin. A full derivation of **Equation 14** can be found in Section 7 (Equations 77 to 91) of the supplement for Salimijazi *et al.* [Salimijazi2020b].

The NAD(P)H, ATP and Fd<sub>red</sub> requirements for lixiviant synthesis were calculated by balancing networks of reactions for the autotrophic synthesis of the molecule from CO<sub>2</sub> or formate (COOH<sup>-</sup>). We enumerated all reaction steps for the production of 4 environmentally benign lixiviant molecules (acetic, citric, 2,5-diketo-gluconic, and gluconic acid) from acetyl-CoA and using data from the KEGG database in **Table S2** [Kanehisa2000a, Kanehisa2019a, Kanehisa2021a].

Lixiviant synthesis reactions were complemented with reactions for CO<sub>2</sub>-fixation and C<sub>1</sub>-assimilation. For this article we considered 6 scenarios in which CO<sub>2</sub> was fixed by the well-known Calvin cycle [Berg2002a], the Reductive Tricarboxylic Acid cycle [Alissandratos2015a, Claassens2016a], Wood-Ljungdahl (WL) Pathway [Berg2002a]; the 3-hydroxypropionate/4-hydroxybutyrate (3HP-4HB) Pathway [BergI2007a, Claassens2016a]; 3-hydroxypropionate (3HP) Cycle [Zarzycki2009a]; and the Dicarboxylate/4-hydroxybutyrate (4HB) Cycle [Huber2008a]. In addition, we also considered the artificial Formolase formate assimilation pathway [Siegel2015a]. These reactions can be found in **Table S3**.

The CO<sub>2</sub>-fixation and C<sub>1</sub>-assimilation and lixiviants were combined by hand into a set of stoichiometric matrices),  $\mathbf{S}_{\text{lix}}$ , for each reaction network. Stoichiometric matrices are included in **Dataset S1**. Stoichiometric matrices were balanced with a custom flux balance program [Barstow2021b] to find the overall stoichiometry for synthesis of each lixiviant using each CO<sub>2</sub>-fixation or C<sub>1</sub>-assimilation pathway. The balanced overall stoichiometry for synthesis of each lixiviant by each CO<sub>2</sub> fixation or C<sub>1</sub> assimilation pathway can be found in **Table S4**.



## Results and Discussion

### Mass of Lixiviants Needed for Global Scale CO<sub>2</sub> Sequestration Can Outstrip Global Supply When De-mineralization Efficiencies Are Low

We plot the mass of lixiviant required for the sequestration of 20 GtCO<sub>2</sub> per year (the amount of CO<sub>2</sub> that will need to be sequestered per year in the late 21<sup>st</sup> century [ipcc2018a]) as a function of the product of the inverse CO<sub>2</sub> mineralization performance,  $\zeta$ , in **Figure 2**.

What range of values could we expect for the CO<sub>2</sub> mineralization efficiency? To estimate  $\zeta$  we have made educated guesses for each of the values from the scientific literature. At the optimistic end of the spectrum, we assume that the concentration of lixiviant is 100 mM (corresponding to  $\approx$  pH 2.1 for citric acid, pH 2.4 for gluconic acid, and pH 2.9 for acetic acid; **Note S1**), the extraction and the precipitation efficiency are both 100%, and the pulp density is 50% w/v (500,000 g m<sup>-3</sup>) [MacDonald2007a],

$$\begin{aligned}\zeta_{\text{optimistic}} &= 100 \text{ Mol m}^{-3} / (1 \times 1 \times 5 \times 10^5 \text{ g m}^{-3}) \\ &= 2 \times 10^{-4} \text{ Mol g}^{-1}.\end{aligned}\tag{15}$$

The optimistic value of  $\zeta$  is marked as the furthest left vertical line in **Figure 2**, and corresponds to a consumption of 1.26 Gt of dry lixiviant per year. Even this optimistic scenario corresponds to a significant amount of biomass, accounting for 90% of US biomass production [Perlack2011a] even if cellulosic biomass could be converted to lixiviant with 100% mass conversion efficiency.

What are the consequences for lixiviant demand if some of the factors included in  $\zeta$  are slightly less than the optimistic estimates? If just the lixiviant concentration,  $c_{\text{lix}}$ , increases by only 10%, or any one of the denominator factors in  $\zeta$  ( $\eta_{\text{ex}}$ ,  $\eta_{\text{precip}}$ ,  $\rho_{\text{pulp}}$ ) decreases by 10%, the minimum mass of lixiviant required to sequester 20 GtCO<sub>2</sub> will rise to 1.4 Gt, equal to the entire biomass production of the United States [Perlack2011a] (**Figure 2**, second vertical line from the left). The same increase in  $\zeta$  can be achieved by a simultaneous 3% increase in  $c_{\text{lix}}$ , and 3% reduction in  $\eta_{\text{ex}}$ ,  $\eta_{\text{precip}}$ , and  $\rho_{\text{pulp}}$ . We have calculated possible combinations of values of  $c_{\text{lix}}$ ,  $\eta_{\text{ex}}$ ,  $\eta_{\text{precip}}$ , and  $\rho_{\text{pulp}}$  that produce each of the values of  $\zeta$  highlighted in **Figure 2** in **Table S5**.

What are the consequences for lixiviant demand if one or more of the factors in  $\zeta$  are significantly less than the optimistic estimates? Slade *et al.* [Slade2014a] calculated the effects of withdrawing increasing quantities of bio-energy from the biosphere. We can make an approximate conversion from bio-energy to dry weight of biomass by dividing by the energy density of dry cellulosic material,

$$M_{\text{biomass}} \approx \frac{E_{\text{biomass}}}{\rho_{\text{energy, dry cellulose}}}.\tag{X}$$

Slade *et al.* [Slade2014a] identified 3 transition points with increasingly restrictive consequences for global civilization (including a combination of crop yield increases, and population, diet and forestry control) that come with increasing biomass use. We have marked these transition points as the third, fourth and fifth horizontal lines from the bottom of **Figure 2**. We have marked values of  $\zeta$  that correspond to these transition points as the third, fourth and fifth vertical lines from the left in **Figure 2**.

A significant change in one of the factors of  $\zeta$  or two smaller simultaneous changes is required for lixiviant demand to pass the first consequential transition identified by Slade *et al.* [Slade2014a]. The first transition occurs when the withdrawal of bio-energy from the biosphere exceeds 100 exajoules per year (EJ) (corresponding to  $\approx 7$  Gt of dry biomass). Exceeding this withdrawal rate will require that crop yields keep pace with demand; and either adoption of vegetarian diets, or a low global population ( $< 9$  billion), or limited deforestation. Increasing the lixiviant demand rate to  $\approx 7$  Gt per year occurs when  $\zeta$  rises to  $1 \times 10^{-6}$  Mol g<sup>-1</sup>. This increase in  $\zeta$  will happen if  $c_{\text{lix}}$  rises by a factor of  $\approx 5$  to 530 mM, or a reduction in any one of the of the denominator factors ( $\eta_{\text{ex}}$ ,  $\eta_{\text{precip}}$ , and  $\rho_{\text{pulp}}$ ) to  $\approx 1/5^{\text{th}}$  of its optimistic value (**Figure 2**, **Table S5**).  $\zeta$  can also rise to  $10^{-6}$  Mol g<sup>-1</sup> if  $c_{\text{lix}}$  rises by a factor of  $\approx 2$ , and one of the denominator factors falls to  $\approx 1/2$  of its optimistic value, or two of the the denominator factors fall to  $\approx 1/2$  of their optimistic value. Alternatively, the same increase in  $\zeta$  can also happen if  $c_{\text{lix}}$  increases by  $\approx 50\%$  ( $3/2$ ), and the denominator factors all decrease to about  $2/3^{\text{rds}}$  of their optimistic values (**Table S5**).

Significant changes in two factors contributing to  $\zeta$  are required for lixiviant demand to pass the second consequential transition identified by Slade *et al.* [Slade2014a]. This second transition occurs when the withdrawal of bio-energy from the biosphere exceeds 300 EJ per year ( $\approx 20$  Gt of dry biomass per year). Exceeding this withdrawal rate will require that increases in crop yields outpace demand; and either adoption of vegetarian diets, a low population or limited deforestation. Increasing the lixiviant demand rate to 20 Gt occurs if there are simultaneous reductions in two of the three denominator factors of  $\zeta$  to  $\approx 1/4^{\text{th}}$  of their optimistic value, or an increase in  $c_{\text{lix}}$  to  $\approx 400$  mM (a factor of 4) (**Figure 2** and **Table S5**). Alternatively, a doubling of  $c_{\text{lix}}$  to  $\approx 200$  mM, and a reduction in all the denominator factors to  $1/2$  their optimistic value will also raise lixiviant demand to 20 Gt (**Table S5**).

Significant changes in three factors contributing to  $\zeta$  are required for lixiviant demand to pass the third consequential transition identified by Slade *et al.* [Slade2014a]. The third transition point occurs when bio-energy withdrawal exceeds 600 EJ yr<sup>-1</sup> ( $\approx 40$  Gt of dry biomass per year). Exceeding this withdrawal rate requires high input farming, high increases in crop yields, limiting global population to  $< 9$  billion, and adoption of either vegetarian diets or managed forestry [Slade2014a]. Increasing the lixiviant demand rate to 40 Gt can occur if  $c_{\text{lix}}$  triples to 300 mM, and 2 of the denominator factors are reduced to  $\approx 1/3^{\text{rd}}$  of their optimistic values (**Figure 2** and **Table S5**).

Finally, the lixiviant demand rate can thoroughly bust the Earth's biomass budget, exceeding net primary productivity (NPP) of 120 EJ yr<sup>-1</sup> (80 Gt dry biomass) if  $c_{\text{lix}}$  increases to 280 mM, and all 3 denominator factors are reduced to  $\approx 1/3^{\text{rd}}$  of their optimistic values (**Figure 2** and **Table S5**).

Taken together, the results presented here suggest that CO<sub>2</sub> mineralization accelerated with biologically produced lixiviants could (although this is definitely not guaranteed) place an undesirable burden on the Earth's biosphere.

### **Electromicrobial Production Could Produce Lixiviants at a Cost of a Few Hundred Dollars per Tonne**

Electromicrobial production technologies already have lab scale efficiencies that can exceed the theoretical upper limit efficiencies of most forms of photosynthesis [Torella2015a, Liu2016a, Haas2018a], and have even further room to improve [Salimijazi2020b, Wise2021a]. This means that electromicrobial production might be able to produce lixiviants for CO<sub>2</sub> mineralization from electricity and CO<sub>2</sub> without needing to compete for land with agriculture and wilderness.



We used our theory of electromicrobial production (**Theory** and refs [Salimijazi2020b, Wise2021a]) to calculate the minimum electricity needs, and hence minimum solar electricity costs needed to produce a tonne of 4 different lixiviant compounds: acetic acid, citric acid, 2,5-diketogluconic acid, and gluconic acid (**Figure 3**).

The most expensive lixiviant to synthesize is acetic acid produced with the 4HB CO<sub>2</sub>-fixation pathway and with electrons supplied with extracellular electron uptake (EEU) at a cost of  $56.2_{-1.9}^{+6.8}$  kJ g<sup>-1</sup>. Assuming that the US Department of Energy's solar PV electricity price projection for 2030 of 3 ¢ per kilowatt-hour can be achieved, this translates to a cost of \$468 per tonne of acetic acid (right hand side axes in **Figure 3**).

As in our earlier analyses [Salimijazi2020b, Wise2021a] modifying the CO<sub>2</sub> fixation method from the least efficient (the 4HB pathway) to the most efficient (the Wood-Ljungdahl pathway) can reduce energy costs of electromicrobial production by almost a factor of 2 [Salimijazi2020b, Wise2021a]. Likewise, switching the electron delivery mechanism to H<sub>2</sub>-oxidation further reduces energy costs of production. The lowest cost method for producing acetic acid is with the Wood-Ljungdahl CO<sub>2</sub>-fixation pathway and with electrons supplied by H<sub>2</sub>-oxidation, which results in a cost of  $25.7_{-0}^{+0}$  kJ g<sup>-1</sup>, or \$214 per tonne. The lowest cost lixiviant is citric acid, with a minimum cost of  $21.1_{-0.5}^{+0.1}$  kJ g<sup>-1</sup> (\$175 per tonne) when produced with the Wood-Ljungdahl pathway and with electron delivery by H<sub>2</sub>-oxidation.

Electromicrobial lixiviant production is more expensive than biomass production, even with projected 2030 solar PV prices, but might still achieve cost parity. The farm gate cost of cellulosic biomass ranges from \$39.7/dry tonne for loblolly pine wood chip to \$72.3/dry tonne for switchgrass [Liu2015a], between 3 and 10 times cheaper than electromicrobially produced lixiviants. However, these costs do not include the cost of conversion of cellulosic biomass to a lixiviant. It is estimated that the production cost of cellulosic ethanol is \$2.65 per US gallon (\$890 per tonne), and it is reasonable to assume that lixiviant production would incur similar costs. Electromicrobial production of lixiviants could still achieve cost parity with biomass-derived lixiviants by directly producing the lixiviant and avoiding conversion costs.

### **Electromicrobially Produced Lixiviants Might Enable Cost-competitive CO<sub>2</sub> Mineralization**

The costs of CO<sub>2</sub> mineralization with electromicrobially produced lixiviants are high, but could still enable cost effective CO<sub>2</sub> mineralization. We have plotted the amount of energy needed to synthesize enough acetic, gluconic, citric and 2,5-diketo-gluconic acid to sequester 1 tonne of CO<sub>2</sub> as a function of the inverse CO<sub>2</sub> mineralization economy,  $\zeta$ , in **Figure 4**. While acetic acid is the most expensive lixiviant to produce on a per tonne basis, for a given value of  $\zeta$ , it produces the lowest cost CO<sub>2</sub> mineralization.

For the most optimistic value of  $\zeta$  ( $2 \times 10^{-4}$  Mol g<sup>-1</sup>), the cost of electricity (at projected 2030 PV prices) needed to make enough gluconic acid to sequester 1 tonne of CO<sub>2</sub> is \$17 (and only \$6 for acetic acid) (**Figure 4**). Even when  $\zeta$  rises to  $1 \times 10^{-3}$  Mol g<sup>-1</sup> (corresponding to a biomass drain from the biosphere that would prompt significant changes to global agriculture) the cost of sequestering a tonne of CO<sub>2</sub> only rises to \$87 when using gluconic acid, and \$30 when using acetic acid (**Figure 4**).

## Conclusions

CO<sub>2</sub> sequestration at the scale discussed in this article (20 GtCO<sub>2</sub> yr<sup>-1</sup>) is not likely to be needed for approximately 50 years from the time of writing (around 2070). This means that there is time to identify technologies that could meet this need and refine them to do it. Weathering of ultramafic rocks and subsequent mineralization of CO<sub>2</sub> almost certainly has the capacity to deal with the excess CO<sub>2</sub> in the atmosphere, but accelerating this process remains a challenge.

Accelerating the weathering of ultramafic materials to the rate necessary to keep climate change within acceptable limits with organic lixiviants made from cellulosic biomass has the potential to monopolize the world's biomass supply. Even under the most optimistic estimate of CO<sub>2</sub> mineralization performance, sequestration of 20 GtCO<sub>2</sub> per year could use 90% of the biomass production of the entire United States (**Figure 2**). If the CO<sub>2</sub> mineralization performance were to slip slightly, accelerated CO<sub>2</sub> mineralization could force undesirable changes to the world agricultural system and society (**Figure 2**).

Electromicrobial production of organic lixiviants could enable accelerated CO<sub>2</sub> mineralization without competing for agricultural land. While EMP technologies only exist in the lab today, their high lab-scale and even higher predicted solar to product conversion efficiencies mean that they could be an effective tool in CO<sub>2</sub> management. In this article, we demonstrate that organic lixiviants can be produced by EMP at the cost of ≈ \$200 to \$400 per tonne assuming solar electricity is supplied at a cost of 3¢ per kWh (a target for 2030 solar electricity costs set by the US Department of Energy [SunShot]) (**Figure 3**).

Electromicrobially produced lixiviants could enable large scale CO<sub>2</sub> mineralization at low costs. We show that even with modest CO<sub>2</sub> mineralization performance, the cost of making the lixiviants needed to sequester a tonne of CO<sub>2</sub> could be kept below \$100 per tonne, even with 2030 solar electricity costs (**Figure 4**). It is highly likely that many more halvings of solar electricity cost will occur between 2030 and 2070, further reducing the cost of CO<sub>2</sub> mineralization.

What's the best way to achieve the potential of EMP for CO<sub>2</sub> mineralization? Until recently, the difficulty of adding CO<sub>2</sub> fixation to a non-CO<sub>2</sub>-fixing organism; uncertainty about the efficiency of electron uptake by EET and even if it can reduce the NADH needed for CO<sub>2</sub> fixation; and the difficulty of engineering non-model organisms like *G. oxydans* has made a project like this look unfeasible. However, recently Rowe *et al.* [Rowe2018a] discovered that *S. oneidensis* can use imported electrons to reduce NADH. Meanwhile, Gleizer *et al.* [Gleizer2019a] transformed the lab workhouse microbe *E. coli* to fix CO<sub>2</sub>.

Furthermore, we have recently discovered the genes that code for this electron uptake pathway in the electroactive microbe in *S. oneidensis*; and have used the Knockout Sudoku technology [Baym2016a, Anzai2017a] to build a whole genome knockout collection of the mineral-dissolving microbe *G. oxydans*, the first step in whole genome engineering. Added together these breakthroughs make something that appeared almost impossible a year ago look tantalizingly close.

## **End Notes**

### **Code Availability**

All code used in calculations in this article is available at <https://github.com/barstowlab/electroCO2> and is archived on Zenodo [Barstow2021b].

### **Materials & Correspondence**

Correspondence and material requests should be addressed to B.B.

### **Author Contributions**

Conceptualization, B.B.; Methodology, B.B. and S.M.; Investigation, S.M., A.D., L.G., L.L., K.S., I.T., J.Z., and B.B; Writing - Original Draft, A.D., L.G., L.L., K.S., I.T., J.Z., and B.B.; Writing - Review and Editing, B.B.; Resources, B.B.; Supervision, B.B..

### **Acknowledgements**

This work was supported by Cornell University startup funds, a Career Award at the Scientific Interface from the Burroughs Wellcome Fund, ARPA-E award DE-AR0001341, and by U.S. Department of Energy Biological and Environmental Research grant DE-SC0020179 to B.B..

### **Competing Interests**

The authors declare no competing interests.

## Figures

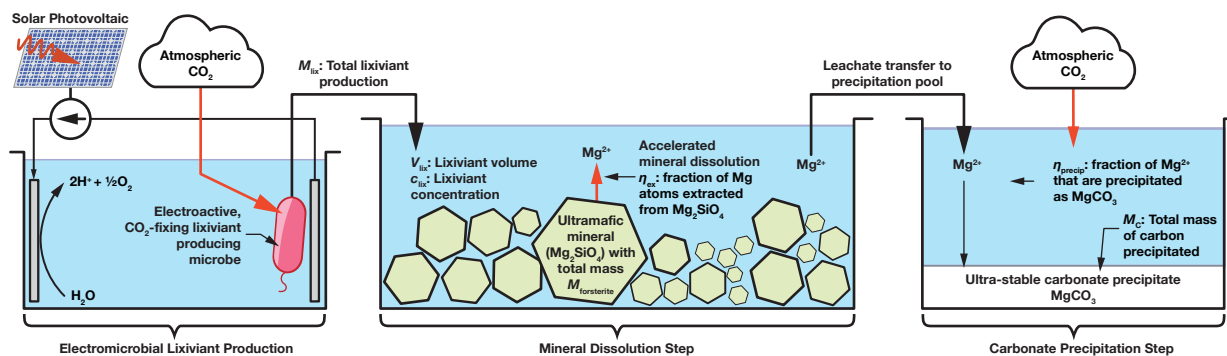


**Figure 1.** Overview of electromicrobially accelerated CO<sub>2</sub> mineralization process. Key parameters in this article are highlighted in this figure, **Figure 2**, and **Tables 1** and **2**.

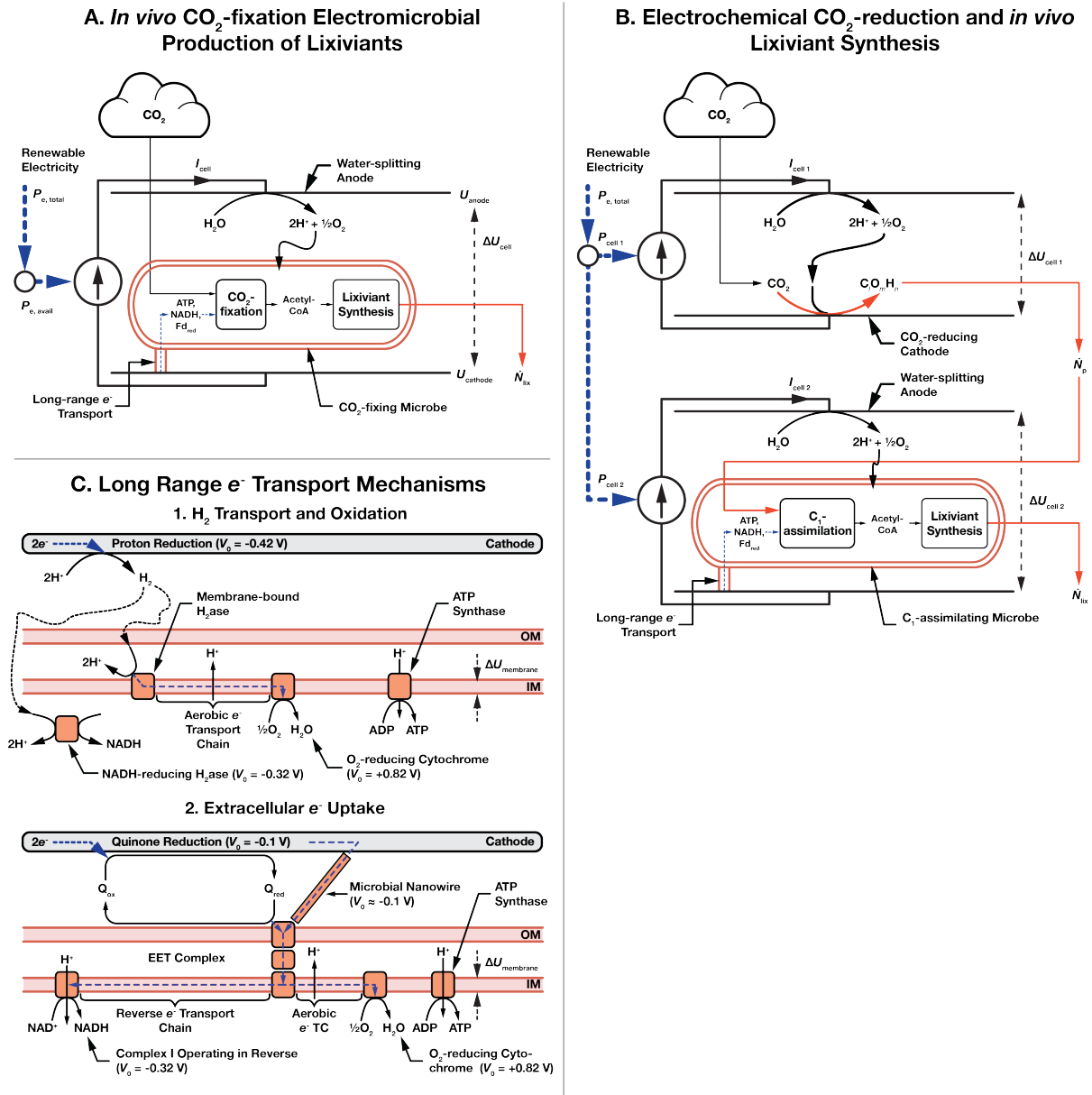


**Figure 2.** Schematic of electromicrobial production of lixivants for CO<sub>2</sub> mineralization. **(A)** Single bioelectrochemical cell system where electricity is used to power *in vivo* CO<sub>2</sub>- and subsequent lixiviant synthesis. **(B)** Dual electrochemical cell system where CO<sub>2</sub> is reduced in the first cell, and then assimilated in the second cell to produce lixiviant molecules. **(C)** Long range e<sup>-</sup> transfer mechanisms considered in this article. In the first, H<sub>2</sub> is electrochemically reduced on a cathode, transferred to the microbe by diffusion or stirring, and is enzymatically oxidized. In the second mechanism, extracellular electron uptake (EEU), e<sup>-</sup> are transferred along a microbial nanowire (part of a conductive biofilm), or by a reduced medium potential redox shuttle like a quinone or flavin, and are then oxidized at the cell surface by the extracellular electron transfer (EET) complex. From the thermodynamic perspective considered in this article, these mechanisms are equivalent. Electrons are then transported to the inner membrane where reverse electron transport is used to regenerate NAD(P)H, reduced Ferredoxin (not shown), and ATP [Rowe2018a, Rowe2021a]. Parameters for these systems are shown in **Table 2**.

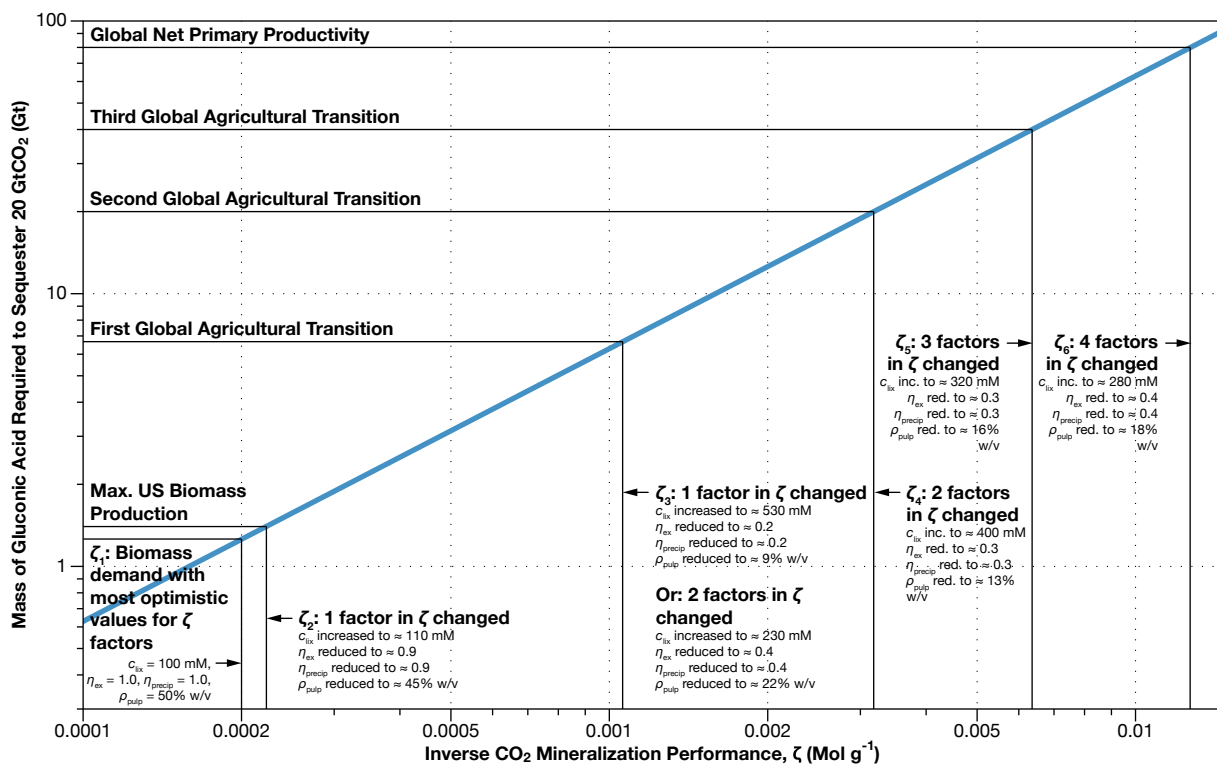


**Figure 3.** Accelerated mineralization could require hundreds of millions to tens of billions of tonnes of lixivants per year. If these lixivants were produced from cellulosic biomass, this could put a significant strain on the world agricultural system. We calculated the mass of lixiviant ( $M_{lix}$ ) needed to accelerate the dissolution step of mineralization of 20 GtCO<sub>2</sub> per year using **Equation 10** as a function of the inverse CO<sub>2</sub> mineralization performance,  $\zeta$ , the combination of the most uncertain parameters in our estimate of lixiviant mass. We chose to display results for gluconic acid as it has the highest molecular weight and provides an upper bound on the lixiviant mass requirement. Our most optimistic estimate for  $\zeta$  ( $\zeta_1$ ) is shown as the left most vertical line on the plot. The second marked value of  $\zeta$  ( $\zeta_2$ ) corresponds to a mass of lixiviant equal to all of the cellulosic biomass produced in the United States in a year. The third, fourth and fifth lines ( $\zeta_3$  to  $\zeta_5$ ) correspond to increasing biomass withdrawals from the biosphere that come with increasingly severe consequences for agriculture and human society including adoption of vegetation diets, population control and widespread managed agriculture and forestry [Slade2014a]. The sixth ( $\zeta_6$ ) and final line corresponds to the biomass production of the entire world in a year (net primary productivity). This plot can be reproduced with the NLIXIVANT.PY code in the ELECTROCO2 repository [Barstow2021b].



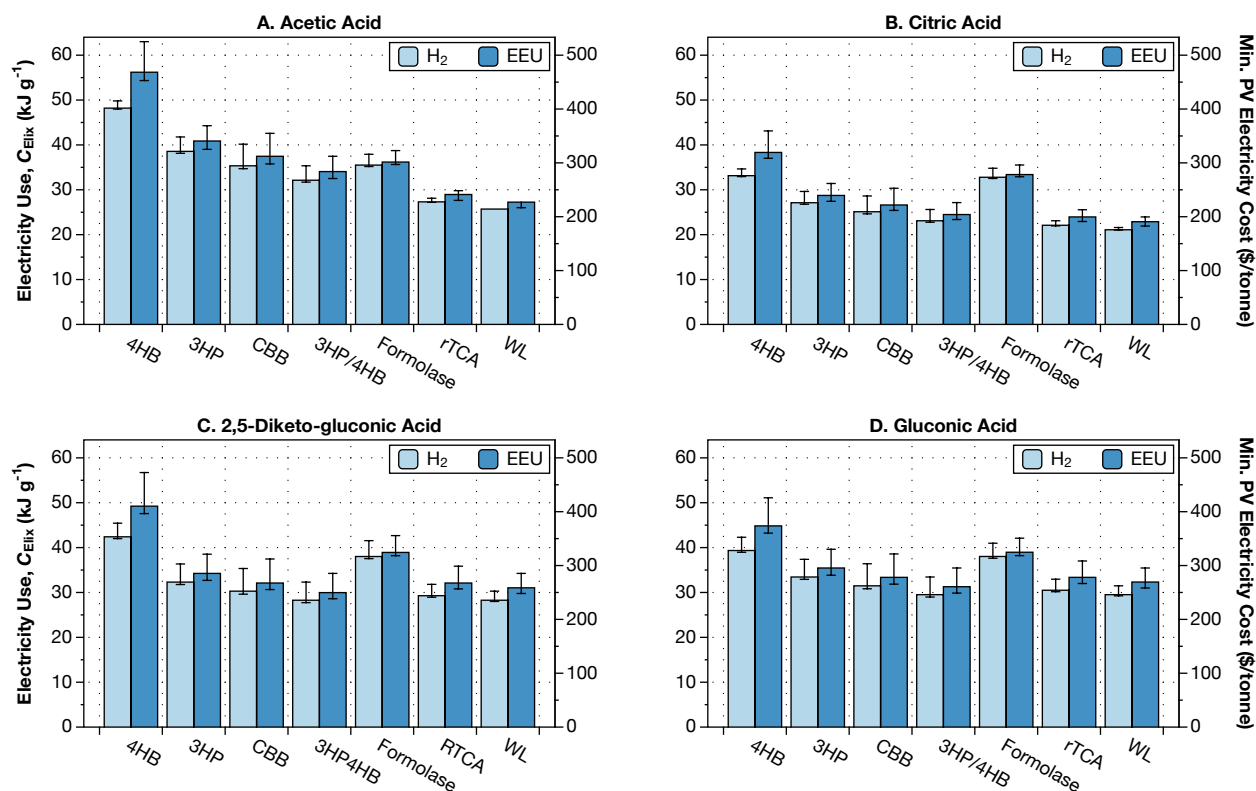


**Figure 4.** Electromicrobial production technology could reduce the electrical energy costs of lixiviant production to a few tens of kilojoules per gram. Energy and financial costs for producing 4 lixiviant molecules are shown in each panel: (A) acetic acid, (B) citric acid, (C) 2,5-diketo-gluconic acid (DKG), and (D) gluconic acid. The electrical energy cost of producing a gram of each lixiviant is shown the left hand side y-axis for each sub-plot. The dollar cost of producing a tonne of the lixiviant using electricity supplied by solar photovoltaics at a cost of 3¢ per kWh (the US Department of Energy’s cost target for solar electricity for 2030 [SunShot]). This plot can be reproduced using the EFFICIENCY.PY code in the ELECTROCO2 repository [Barstow2021b].

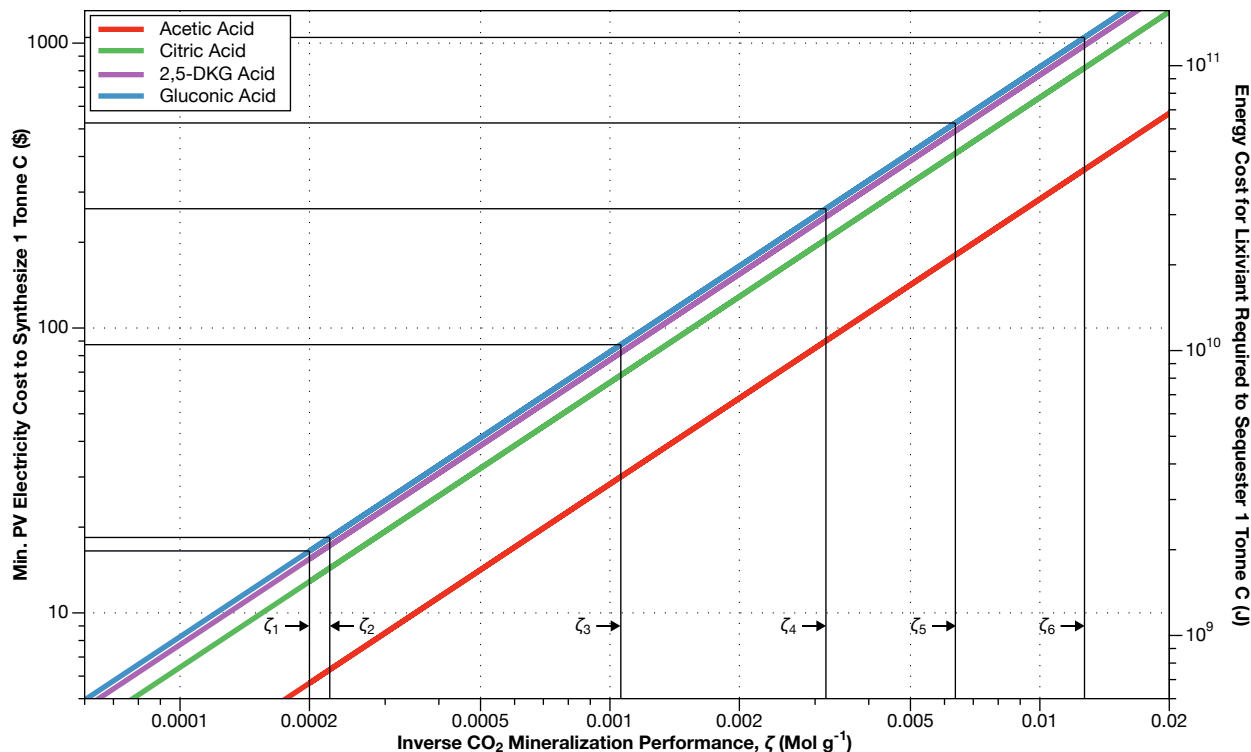


**Figure 5.** Electromicrobial production technology could enable production of enough lixiviants to sequester 1 tonne of CO<sub>2</sub> for less than \$100. We combined our lixiviant mass requirements from **Figure 3**, with our estimates for the energy and financial cost of producing a tonne of each lixiviant compound with H<sub>2</sub>-mediated EMP using CO<sub>2</sub>-fixation with the Calvin cycle (basically the Bionic Leaf configuration [Torella2015a, Liu2016a]) from **Figure 4**. For illustrative purposes we have marked the values of the inverse CO<sub>2</sub> mineralization performance ( $\zeta_1$  to  $\zeta_6$ ) highlighted in **Figure 3**, and the corresponding cost to sequester a tonne of CO<sub>2</sub> as an intersecting horizontal line. However, it is important to note that in this case, no cellulosic biomass is produced. This plot can be reproduced using the CLIXIVIAN.PY code in the ELECTROCO<sub>2</sub> repository [Barstow2021b].

Symbol	Unit	Description
$\dot{N}_{lix}$	molecule s <sup>-1</sup>	Lixiviant molecules produced per second by electromicrobial production system.
$N_A$	Mol <sup>-1</sup>	Avogadro constant
F	A s Mol <sup>-1</sup>	Faraday constant
$P_{e, total}$	J s <sup>-1</sup>	Total electrical power input into electromicrobial production system.
$MW_{lix}$	g Mol <sup>-1</sup>	Molecular weight of the lixiviant molecule.
$e$	A s	Fundamental charge
$v_{elix}$	#	Number of electrons needed for synthesis of a lixiviant molecule from CO <sub>2</sub> .
$\Delta U_{cell}$	V	Potential difference across bio-electrochemical cell.
$v_{elix, add}$	#	Number of electrons needed to convert a C <sub>1</sub> compound to a lixiviant molecule.
$v_r$	#	Number of primary reduction products to make a molecule of final product.
$v_{er}$	#	Number of electrons to reduce CO <sub>2</sub> to a primary reduction product.
$v_{Cr}$	#	Number of carbon atoms per primary reduction product.
$\zeta_{I2}$	#	Faradaic efficiency of the bio-electrochemical cell.
$\zeta_{I1}$	#	Faradaic efficiency of the primary abiotic cell.
$\zeta_C$	#	Carbon transfer efficiency from cell 1 to cell 2.
$v_{lix, NADH}$	#	Number of NAD(P)H molecules needed to make a lixiviant molecule.
$v_p, Fd$	#	Number of Fd molecules needed to make a lixiviant molecule.
$v_p, ATP$	#	Number of ATP molecules needed to make a lixiviant molecule.
$\Delta G_{ATP/ADP}$	J	Free energy for regeneration of ATP
$\Delta U_{membrane}$	V	Inner membrane potential difference.
$U_{H2}$	V	Standard potential of proton reduction to H <sub>2</sub> .
$U_{acceptor}$	V	Standard potential of terminal electron acceptor reduction.
$U_Q$	V	Redox potential of the inner membrane electron carrier.
$U_{NADH}$	V	Standard potential of NADH
$U_{Fd}$	V	Standard potential of Ferredoxin
$C_{Elix}$	J g <sup>-1</sup>	Electrical energy cost per unit mass of lixiviant.
$C_{Slix}$	¢ g <sup>-1</sup>	Solar energy cost per unit mass of lixiviant.
$V_{forsterite}$	m <sup>3</sup>	Volume of forsterite needed to capture $M_C$ of carbon.
$C_{lix}$	Mol m <sup>-3</sup>	Concentration of lixiviant used to dissolve forsterite.
$V_{lix}$	m <sup>3</sup>	Volume of lixiviant used to dissolve forsterite.
$\rho_{pulp}$	#	Pulp density. Ratio of forsterite to lixiviant volumes.
$\eta_{precip}$	#	Precipitation efficiency. Percentage of ions in leachate that are incorporated into magnesite.
$\eta_{ex}$	#	Extraction efficiency. Percentage of Mg atoms in forsterite that are released into leachate solution.
$n_C, olivine$	#	Maximum number of C atoms that can be sequestered per asymmetric unit of forsterite dissolved.
$MW_{forsterite}$	g Mol <sup>-1</sup>	Molecular weight of forsterite (140.69).
$\zeta$	Mol m <sup>-3</sup>	Aggregated high uncertainty terms mass of lixiviant calculation.
$M_{lix}$	g	Dry mass of lixiviant needed to sequester $M_C$ of carbon as magnesite.
$M_C$	g yr <sup>-1</sup>	Mass of C (not CO <sub>2</sub> ) to be sequestered (10 <sup>13</sup> g yr <sup>-1</sup> ). Multiply by 44/12 to calculate mass of CO <sub>2</sub> .

**Table 1.** Symbols used in this article.

Parameter	Symbol	1. H <sub>2</sub>	2. EEU	3. H <sub>2</sub> with Formate	4. EEU with Formate
<b>Electrochemical Cell Parameters</b>					
Input solar power (W)	$P_{\gamma}$	1,000	1,000	1,000	1,000
Total available electrical power (W)	$P_{e, total}$	330	330	330	330
CO <sub>2</sub> -fixation method		Enzymatic		Electrochemical	
Electrode to microbe mediator		H <sub>2</sub>	EEU	H <sub>2</sub>	EEU
Cell 1 cathode std. potential (V)	$U_{cell 1, cathode, 0}$	N/A		0.82 [Torella2015a]	
Cell 1 cathode bias voltage (V)	$U_{cell 1, cathode, bias}$	N/A		0.47 [Liu2016a]	
Cell 1 anode std. potential (V)	$U_{cell 1, anode, 0}$	N/A		-0.43 [Yishai2017a, Zhang2018a]	
Cell 1 anode bias voltage (V)	$U_{cell 1, anode, bias}$	N/A		1.3 [White2014a]	
Cell 1 voltage (V)	$\Delta U_{cell 1}$	N/A		3.02	
Cell 1 Faradaic efficiency	$\zeta_{11}$	N/A		0.8 [Rasul2019a]	
Carbons per primary fixation product	$\nu_{Cr}$	N/A		1	
$e^-$ per primary fixation product	$\nu_{er}$	N/A		2	
Cell 2 (Bio-cell) anode std. potential (V)	$U_{cell 2, anode, 0}$	-0.41 [Torella2015a]	-0.1 [Bird2011a, Firer-Sherwood2008a]	-0.41	-0.1
Bio-cell anode bias voltage (V)	$U_{cell 2, anode, bias}$	0.3 [Liu2016a]	0.2 [Uek2018a]	0.3	0.2
Bio-cell cathode std. potential (V)	$U_{cell 2, cathode, 0}$	0.82			
Bio-cell cathode bias voltage (V)	$U_{cell 2, cathode, bias}$	0.47			
Bio-cell voltage (V)	$\Delta U_{cell 2}$	2 [Liu2016a]	1.59	2	1.59
Bio-cell Faradaic efficiency	$\zeta_{12}$	1.0			
<b>Cellular Electron Transport Parameters</b>					
Membrane potential difference (mV)	$\Delta U_{membrane}$	140		140	
Terminal $e^-$ acceptor potential (V)	$U_{Acceptor}$	0.82			
Quinone potential (V)	$U_Q$	-0.0885 [Bird2011a]		-0.0885 [Bird2011a]	
Mtr EET complex potential (V)	$U_{Mtr}$	N/A	-0.1 [Salimijazi2020b]	N/A	-0.1 [Salimijazi2020b]
No. protons pumped per $e^-$	$p_{out}$	Unlimited		Unlimited	
<b>Product Synthesis Parameters</b>					
No. ATPs for product synthesis	$\nu_{p, ATP}$	See <b>Table S4</b>			
No. NAD(P)H for product	$\nu_{p, NADH}$	See <b>Table S4</b>			
No. Fd <sub>red</sub> for product	$\nu_{p, Fd}$	See <b>Table S4</b>			

**Table 2.** Electromicrobial lixiviant production model parameters. Model parameters used in this article are based upon model parameters used in a previous analysis of the electromicrobial production of the biofuel butanol [Salimijazi2020b]. A sensitivity analysis was performed for all key parameters in this work [Salimijazi2020b].

## References

- [Alissandratos2015a] A. Alissandratos and C. J. Easton. “Biocatalysis for the application of CO<sub>2</sub> as a chemical feedstock”. *Beilstein Journal of Organic Chemistry* 11 (2015), pp. 2370–2387. doi: [10.3762/bjoc.11.259](https://doi.org/10.3762/bjoc.11.259).
- [Anzai2017a] I. A. Anzai, L. Shaket, O. Adesina, M. Baym, and B. Barstow. “Rapid curation of gene disruption collections using Knockout Sudoku”. *Nature Protocols* 12.10 (2017), p. 2110 2137. doi: [10.1038/nprot.2017.073](https://doi.org/10.1038/nprot.2017.073).
- [Archer2009a] D. Archer, M. Eby, V. Brovkin, A. Ridgwell, L. Cao, U. Mikolajewicz, K. Caldeira, K. Matsumoto, G. Munhoven, A. Montenegro, and K. Tokos. “Atmospheric Lifetime of Fossil Fuel Carbon Dioxide”. *Annual Review of Earth and Planetary Sciences* 37.1 (2009), pp. 117–134. doi: [10.1146/annurev.earth.031208.100206](https://doi.org/10.1146/annurev.earth.031208.100206).
- [Barstow2015a] B. Barstow. “Molecular Mechanisms for the Biological Storage of Renewable Energy”. English. *Advanced Science, Engineering and Medicine* 7 (2015), pp. 1066–1081. doi: [10.1166/asem.2015.1813](https://doi.org/10.1166/asem.2015.1813).
- [Barstow2021b] B. Barstow. *ElectroCO2 Release for Zenodo*. Zenodo, Dec. 2021. doi: [10.5281/zenodo.5805345](https://doi.org/10.5281/zenodo.5805345).
- [Baym2016a] M. Baym, L. Shaket, I. A. Anzai, O. Adesina, and B. Barstow. “Rapid construction of a whole-genome transposon insertion collection for *Shewanella oneidensis* by Knockout Sudoku”. *Nature Communications* 7.1 (2016), p. 13270. doi: [10.1038/ncomms13270](https://doi.org/10.1038/ncomms13270).
- [Beerling2020a] D. J. Beerling, E. P. Kantzas, M. R. Lomas, P. Wade, R. M. Eufrazio, P. Renforth, B. Sarkar, M. G. Andrews, R. H. James, C. R. Pearce, J.-F. Mercure, H. Pollitt, P. B. Holden, N. R. Edwards, M. Khanna, L. Koh, S. Quegan, N. F. Pidgeon, I. A. Janssens, J. Hansen, and S. A. Banwart. “Potential for large-scale CO<sub>2</sub> removal via enhanced rock weathering with croplands”. *Nature* 583.7815 (2020), pp. 242–248. doi: [10.1038/s41586-020-2448-9](https://doi.org/10.1038/s41586-020-2448-9).
- [Berg2002a] J. Berg, J. Tymoczko, and L. Stryer. *Biochemistry*. 5th. New York, NY: W H Freeman, 2002.
- [BergI2007a] I. A. Berg, D. Kockelkorn, W. Buckel, and G. Fuchs. “A 3-Hydroxypropionate/4-Hydroxybutyrate Autotrophic Carbon Dioxide Assimilation Pathway in Archaea”. *Science* 318 (2007), pp. 1782–1786. doi: [10.1126/science.1149976](https://doi.org/10.1126/science.1149976).
- [Bird2011a] L. J. Bird, V. Bonnefoy, and D. K. Newman. “Bioenergetic challenges of microbial iron metabolisms”. *Trends in Microbiology* 19.7 (2011), pp. 330–340. doi: [10.1016/j.tim.2011.05.001](https://doi.org/10.1016/j.tim.2011.05.001).
- [Claassens2016a] N. J. Claassens, D. Z. Sousa, V. A. M. dos Santos, W. M. de Vos, and J. van der Oost. “Harnessing the power of microbial autotrophy”. *Nature Reviews Microbiology* 14 (2016), pp. 692–706. doi: [10.1038/nrmicro.2016.130](https://doi.org/10.1038/nrmicro.2016.130).
- [Claassens2019a] N. J. Claassens, C. A. R. Cotton, D. Kopljar, and A. Bar-Even. “Making quantitative sense of electromicrobial production”. *Nature Catalysis* 2.5 (2019), pp. 437–447. doi: [10.1038/s41929-019-0272-0](https://doi.org/10.1038/s41929-019-0272-0).
- [Firer-Sherwood2008a] M. Firer-Sherwood, G. S. Pulcu, and S. J. Elliott. “Electrochemical interrogations of the Mtr cytochromes from *Shewanella*: Opening a potential window”. *Journal of Biological Inorganic Chemistry* 13.6 (2008), pp. 849–854. doi: [10.1007/s00775-008-0398-z](https://doi.org/10.1007/s00775-008-0398-z).
- [Gleizer2019a] S. Gleizer, R. Ben-Nissan, Y. M. Bar-On, N. Antonovsky, E. Noor, Y. Zohar, G. Jona, E. Krieger, M. Shamshoum, A. Bar-Even, and R. Milo. “Conversion of *Escherichia coli* to Generate All Biomass Carbon from CO<sub>2</sub>”. *Cell* 179.6 (2019), 1255–1263.e12. doi: [10.1016/j.cell.2019.11.009](https://doi.org/10.1016/j.cell.2019.11.009).
- [Haas2018a] T. Haas, R. Krause, R. Weber, M. Demler, and G. Schmid. “Technical photosynthesis involving CO<sub>2</sub> electrolysis and fermentation”. *Nature Catalysis* 1.1 (2018), pp. 32–39. doi: [10.1038/s41929-017-0005-1](https://doi.org/10.1038/s41929-017-0005-1).
- [Huber2008a] H. Huber, M. Gallenberger, U. Jahn, E. Eylert, I. A. Berg, D. Kockelkorn, W. Eisenreich, and G. Fuchs. “A dicarboxylate/4-hydroxybutyrate autotrophic carbon assimilation cycle in the hyperthermophilic *Archaeum Ignicoccus hospitalis*”. *Proceedings of the National Academy of Sciences* 105 (2008), pp. 7851–7856. doi: [10.1073/pnas.0801043105](https://doi.org/10.1073/pnas.0801043105).

- [ipcc2018a] *Global Warming of 1.5°C. An IPCC Special Report on the impacts of global warming of 1.5°C above pre-industrial levels and related global greenhouse gas emission pathways, in the context of strengthening the global response to the threat of climate change, sustainable development, and efforts to eradicate poverty*. Tech. rep. 2018.
- [Kanehisa2000a] M. Kanehisa and S. Goto. “KEGG: Kyoto Encyclopedia of Genes and Genomes”. *eng. Nucleic Acids Research* 28.1 (2000), pp. 27–30. doi: [10.1093/nar/28.1.27](https://doi.org/10.1093/nar/28.1.27).
- [Kanehisa2019a] M. Kanehisa. “Toward understanding the origin and evolution of cellular organisms”. *Protein Science* 28.11 (2019), pp. 1947–1951. doi: [10.1002/pro.3715](https://doi.org/10.1002/pro.3715).
- [Kanehisa2021a] M. Kanehisa, M. Furumichi, Y. Sato, M. Ishiguro-Watanabe, and M. Tanabe. “KEGG: integrating viruses and cellular organisms”. *Nucleic Acids Research* 49.D1 (2020), gkaa970–. doi: [10.1093/nar/gkaa970](https://doi.org/10.1093/nar/gkaa970).
- [Keleman2019a] P. Kelemen, S. M. Benson, H. Pilorgé, P. Psarras, and J. Wilcox. “An overview of the status and challenges of CO<sub>2</sub> storage in minerals and geological formations”. *Frontiers in Climate* 1 (2019), p. 9. doi: [10.3389/fclim.2019.00009](https://doi.org/10.3389/fclim.2019.00009).
- [Leger2021a] D. Leger, S. Matassa, E. Noor, A. Shepon, R. Milo, and A. Bar-Even. “Photovoltaic-driven microbial protein production can use land and sunlight more efficiently than conventional crops”. *Proceedings of the National Academy of Sciences* 118.26 (2021), e2015025118. doi: [10.1073/pnas.2015025118](https://doi.org/10.1073/pnas.2015025118).
- [Lehmann2020a] J. Lehmann and A. Possinger. “Removal of atmospheric CO<sub>2</sub> by rock weathering holds promise for mitigating climate change.” *Nature* 583.7815 (2020), pp. 204–205. doi: [10.1038/d41586-020-01965-7](https://doi.org/10.1038/d41586-020-01965-7).
- [Lips2018a] D. Lips, J. M. Schuurmans, F. Branco Dos Santos, and K. J. Hellingwerf. “Many ways towards ‘solar fuel’: Quantitative analysis of the most promising strategies and the main challenges during scale-up”. *Energy and Environmental Science* 11.1 (2018), pp. 10–22. doi: [10.1039/c7ee02212c](https://doi.org/10.1039/c7ee02212c).
- [Liu2016a] C. Liu, B. Colón, M. Ziesack, P. Silver, and D. Nocera. “Water splitting biosynthetic system with CO<sub>2</sub> reduction efficiencies exceeding photosynthesis”. *Science* 352.6290 (2016), pp. 1210–1213. doi: [10.1126/science.aaf5039](https://doi.org/10.1126/science.aaf5039).
- [Milo2010a] R. Milo, P. Jorgensen, U. Moran, G. Weber, and M. Springer. “BioNumbers - the database of key numbers in molecular and cell biology”. *Nucleic Acids Research* 38 (2010), pp. D750–D753. doi: [10.1093/nar/gkp889](https://doi.org/10.1093/nar/gkp889).
- [NOAA2021a] *Measuring & Analyzing Greenhouse Gases: Behind the Scenes*. [https://gml.noaa.gov/outreach/behind\\_the\\_scenes/gases.html](https://gml.noaa.gov/outreach/behind_the_scenes/gases.html) (Visited on 01/08/2022).
- [Perlack2011a] R. Perlack and B. Stokes. *U.S. Billion-Ton Update: Biomass Supply for a Bioenergy and Bioproducts Industry*. Tech. rep. Oak Ridge, TN: Oak Ridge National Laboratory, 2011.
- [Power2013a] I. M. Power, A. L. Harrison, G. M. Dipple, S. A. Wilson, P. B. Kelemen, M. Hitch, and G. Southam. “Carbon Mineralization: From Natural Analogues to Engineered Systems”. *Reviews in Mineralogy and Geochemistry* 77.1 (2013), pp. 305–360. doi: [10.2138/rmg.2013.77.9](https://doi.org/10.2138/rmg.2013.77.9).
- [Prevoteau2020a] A. PrévotEAU, J. M. Carvajal-Arroyo, R. Ganigué, and K. Rabaey. “Microbial electrosynthesis from CO<sub>2</sub>: forever a promise?” *Current Opinion in Biotechnology* 62 (2020), pp. 48–57. doi: [10.1016/j.copbio.2019.08.014](https://doi.org/10.1016/j.copbio.2019.08.014).
- [Prosekov2018a] A. Y. Prosekov and S. A. Ivanova. “Food security: The challenge of the present”. *Geoforum* 91 (2018), pp. 73–77. doi: [10.1016/j.geoforum.2018.02.030](https://doi.org/10.1016/j.geoforum.2018.02.030).
- [Rabaey2010a] K. Rabaey and R. A. Rozendal. “Microbial electrosynthesis - Revisiting the electrical route for microbial production”. *Nature Reviews Microbiology* 8.10 (2010), pp. 706–716. doi: [10.1038/nrmicro2422](https://doi.org/10.1038/nrmicro2422).
- [Rabaey2011a] K. Rabaey, P. Girguis, and L. K. Nielsen. “Metabolic and practical considerations on microbial electrosynthesis”. *Current Opinion in Biotechnology* 22.3 (2011), pp. 371–377. doi: [10.1016/j.copbio.2011.01.010](https://doi.org/10.1016/j.copbio.2011.01.010).



- [Rasul2019a] S. Rasul, A. Pugnant, H. Xiang, J.-M. Fontmorin, and E. H. Yu. “Low cost and efficient alloy electrocatalysts for CO<sub>2</sub> reduction to formate”. *Journal of CO<sub>2</sub> Utilization* 32.May 2018 (2019), pp. 1–10. doi: [10.1016/j.jcou.2019.03.016](https://doi.org/10.1016/j.jcou.2019.03.016).
- [Reed2016a] D. W. Reed, Y. Fujita, D. L. Daubaras, Y. Jiao, and V. S. Thompson. “Bioleaching of rare earth elements from waste phosphors and cracking catalysts”. *Hydrometallurgy* 166 (2016), pp. 34–40. doi: [10.1016/j.hydromet.2016.08.006](https://doi.org/10.1016/j.hydromet.2016.08.006).
- [Rowe2018a] A. R. Rowe, P. Rajeev, A. Jain, S. Pirbadian, A. Okamoto, J. A. Gralnick, M. Y. El-Naggar, and K. H. Nealson. “Tracking electron uptake from a cathode into *Shewanella* cells: Implications for energy acquisition from solid-substrate electron donors”. *mBio* 9 (2018), pp. 1–19. doi: [10.1128/mBio.02203-17](https://doi.org/10.1128/mBio.02203-17).
- [Salimijazi2019a] F. Salimijazi, E. Parra, and B. Barstow. “Electrical Energy Storage with Engineered Biological Systems”. *Journal of Biological Engineering* 13.38 (2019), pp. 1–21. doi: [10.1186/s13036-019-0162-7](https://doi.org/10.1186/s13036-019-0162-7).
- [Salimijazi2020b] F. Salimijazi, J. Kim, A. M. Schmitz, R. Grenville, A. Bocarsly, and B. Barstow. “Constraints on the Efficiency of Engineered Electromicrobial Production”. *Joule* 4 (2020), pp. 2101–2130. doi: [10.1016/j.joule.2020.08.010](https://doi.org/10.1016/j.joule.2020.08.010).
- [Schmitz2021b] A. M. Schmitz, B. Pian, S. Medin, M. C. Reid, M. Wu, E. Gazel, and B. Barstow. “Generation of a *Gluconobacter oxydans* knockout collection for improved extraction of rare earth elements”. *Nature Communications* 12.1 (2021), p. 6693. doi: [10.1038/s41467-021-27047-4](https://doi.org/10.1038/s41467-021-27047-4).
- [Siegel2015a] J. B. Siegel, A. L. Smith, S. Poust, A. J. Wargacki, A. Bar-Even, C. Louw, B. W. Shen, C. B. Eiben, H. M. Tran, E. Noor, J. L. Gallaher, J. Bale, Y. Yoshikuni, M. H. Gelb, J. D. Keasling, B. L. Stoddard, M. E. Lidstrom, and D. Baker. “Computational protein design enables a novel one-carbon assimilation pathway”. *Proceedings of the National Academy of Sciences* 112 (2015), p. 201500545 6. doi: [10.1073/pnas.1500545112](https://doi.org/10.1073/pnas.1500545112).
- [Slade2014a] R. Slade, A. Bauen, and R. Gross. “Global bioenergy resources”. *Nature Climate Change* 4.2 (2014), nclimate2097. doi: [10.1038/nclimate2097](https://doi.org/10.1038/nclimate2097).
- [Tilman2011a] D. Tilman, C. Balzer, J. Hill, and B. L. Befort. “Global food demand and the sustainable intensification of agriculture”. *Proceedings of the National Academy of Sciences* 108.50 (2011), pp. 20260–20264. doi: [10.1073/pnas.1116437108](https://doi.org/10.1073/pnas.1116437108).
- [Torella2015a] J. P. Torella, C. J. Gagliardi, J. S. Chen, D. K. Bediako, B. Colón, J. C. Way, P. A. Silver, and D. G. Nocera. “Efficient solar-to-fuels production from a hybrid microbial-water-splitting catalyst system”. *Proceedings of the National Academy of Sciences* 112.8 (2015), pp. 2337–2342. doi: [10.1073/pnas.1503606112](https://doi.org/10.1073/pnas.1503606112).
- [White2014a] J. L. White, J. T. Herb, J. J. Kaczur, P. W. Majsztzik, and A. B. Bocarsly. “Photons to formate: Efficient electrochemical solar energy conversion via reduction of carbon dioxide”. *Journal of CO<sub>2</sub> Utilization* 7 (2014), pp. 1–5. doi: [10.1016/j.jcou.2014.05.002](https://doi.org/10.1016/j.jcou.2014.05.002).
- [Wise2021a] L. Wise, S. Marecos, K. Randolph, E. Nshimyumukiza, M. Hassan, J. Strouse, F. Salimijazi, and B. Barstow. “Thermodynamic Constraints on Electromicrobial Protein Production”. *bioRxiv* (2021). doi: [10.1101/2021.11.22.469619](https://doi.org/10.1101/2021.11.22.469619).
- [Yishai2017a] O. Yishai, L. Goldbach, H. Tenenboim, S. N. Lindner, and A. Bar-Even. “Engineered assimilation of exogenous and endogenous formate in *Escherichia coli*”. English. *ACS Synthetic Biology* 6.9 (2017), p. 1722 1731. doi: [10.1021/acssynbio.7b00086](https://doi.org/10.1021/acssynbio.7b00086).
- [Zarzycki2009a] J. Zarzycki, V. Brecht, M. Müller, and G. Fuchs. “Identifying the missing steps of the autotrophic 3-hydroxypropionate CO<sub>2</sub> fixation cycle in *Chloroflexus aurantiacus*”. *Proceedings of the National Academy of Sciences of the United States of America* 106 (2009), p. 21317.
- [Zhang2018a] K. Y. Zhang, Q. Yu, H. Wei, S. Liu, Q. Zhao, and W. Huang. “Long-Lived Emissive Probes for Time-Resolved Photoluminescence Bioimaging and Biosensing”. *Chemical Reviews* 118 (2018), pp. 1770–1839. doi: [10.1021/acs.chemrev.7b00425](https://doi.org/10.1021/acs.chemrev.7b00425).